

Editor, Ocean Science

Email: editorial@copernicus.org

December 22, 2018

Dear Editor:

Thank you for your letter dated December 12 regarding our manuscript entitled **“Could the mesoscale eddies be reproduced and predicted in the northern south China sea: case studies”** (No: os-2018-74), which was submitted to **Ocean Science** for consideration of publication. We have read reviewer’s comments carefully. Following your suggestions, we have gone through the manuscript and made the following changes in the manuscript.

The line-by-line replies for reviewer’s comments are shown in the attachments. The original comments are quoted in Times New Roman (Bold) and our responses are in Times New Roman.

Once again, thank you and reviewer for the time and energy spending on reading our manuscript and providing constructive comments and suggestions, which are very valuable in improving the quality of our manuscript.

Enclosed, please find our updated manuscript and reply to the reviewer’s comments. We hope this version of our manuscript can meet the standard of publication in this journal, and we look forward to receiving further instruction related to this submission.

Sincerely yours

Dazhi Xu

Topic Editor Decision: Publish subject to minor revisions (review by editor) (12 Dec 2018) by John M. Huthnance

Comments to the Author:

Dear Authors

Thank-you for your revisions. I think some of the review comments are “open to interpretation” and so am still asking for some “Minor Revision”. This is for clarity and to include more of what I think the reviewers were asking for. My comments follow here.

Ans: We are very grateful to the editor for the recognition of our work, and we are very grateful for your efforts and time to improve the quality of this article.

Comments

Page 3

Lines 31-32. Better “. . atmosphere, ocean mesoscale eddies are often described . .”

Ans: Thank you. The sentences have been revised in the revised version. (P3, line 31-32)

Lines 39-40. You have added the references but I think Referee 1 wanted a few words about what is learned from these references, e.g. scales resolved (Fu et al), eddy energy and tracking (Morrow and Le Traon), effects on atmosphere (Frenger et al.).

Ans: Thank you for your constructive advice. The sentences have been rewrote to adapt to the added references in the revised version. (P3, line 45-47)

Line 42 (or nearby). I am sure Referee 2 comment 2 wants more text about motivation in your manuscript, not just the references. Their comment is a suggestion for what to include.

Ans: Thank you. These contents have been added in the revised version. (P3, line 37-45)

Page 3 line 51 to Page 4 line 1. Better “. . exhibits significant mesoscale eddy activity (Fig. 2). Many studies have tried to investigate mesoscale eddies in the NSCS . .”

Ans: Thank you. The sentences have been revised in the revised version. (P4, line 61-62)

Page 4

Line 57. “. . recorded evidence . .” (omit “the”)

Ans: Thank you. The word “the” has been deleted in the revised version. (P4, line 67)

Line 72. “. . 2004. Meanwhile, . .”

Ans: Thank you. The sentences have been revised in the revised version. (P5, line 82)

Line 73. “. . disappeared southeast of Hainan . .”

Ans: Thank you. The sentences have been revised in the revised version. (P5, line 83)

Page 5

Lines 78-79. “. . Despite the activities . . NSCS having received . .”

Ans: Thank you. The sentences have been revised in the revised version. (P5, line 87-88)

Line 82. “. . (Oey et al., 2005); they are . .”

Ans: Thank you. The sentences have been revised in the revised version. (P5, line 91)

Line 87. You have added the references suggested by Referee 1. However, I think you also need to comment on what they show (achieve), what is still needed and so how your study helps.

Ans: Thank you. The contents have been added in the revised version. (P6, line 96-103)

Line 88. “. . two typical anticyclonic eddies . .” Are these AE1 and AE2 (not clear as you have re-arranged the text)? Referee 1 (main comment 1) asked why these two particular eddies were chosen; you should say (they ought to be representative, survive long enough to be useful . . . etc.).

Ans: Thank you. The contents have been added in the revised version. (P6, line 104-105)

Page 6

Line 112. “. . System, are also used. . .” It would be better to divide this sentence which is too long.

Ans: Thank you. The sentence has been revised in the revised version. (P7, line 129)

Line 116. “. . used. Three drifters were designed”

Ans: Thank you. The sentence has been revised in the revised version. (P7, line 133-134)

Page 7

Lines 122-126. “. . study as follows: 1) there must be a closed contour on the merged SLA; 2) there must be one maximum or minimum inside the area of the closed contour for anticyclonic or cyclonic eddy; 3) the difference between the extremum and the outermost closed SLA contour; that is, the amplitude of the mesoscale eddy, must be greater than 2 cm; . .”

Ans: Thank you. The sentences have been revised in the revised version. (P8, line 140-144)

Line 136. “weak” -> “weakly”

Ans: Thank you. The word “weak” has been changed to “weakly” in the revised version. (P8, line 153)

Page 8, Line 156. “. . Legates and Willmott (1990). . .”

Ans: Thank you. The expression of the reference has been corrected in the revised version. (P9, line 173-174)

Page 9

Line 176. Please check fonts and alignment for “a”, “b”, “d”.

Ans: Thank you. All formulas and symbols have been rewritten and corrected in the revised version. (P10, line 191-P11, line 205)

Line 179. Likewise fonts for P, R to match symbols in equation (2).

Ans: Thank you. All formulas and symbols have been rewritten and corrected in the revised version. (P10, line 190-P11, line 204)

Page 10.

Line 190. “. . CSCASS are in Li . .”

Ans: Thank you. The sentence has been revised in the revised version. (P11, line 207)

Line 193. “. . reproduction of anticyclonic eddies AE1 and AE2 in the NSCS . .”

Ans: Thank you. The section topic has been revised in the revised version. (P11, line 211)

Lines 197-198. “. . into CSCASS every 3 days . .”

Ans: Thank you. The sentence has been revised in the revised version. (P11, line 214)

Page 11.

Line 209. “. . when the ANP is greater . .”

Ans: Thank you. The sentence has been revised in the revised version. (P12, line 226)

Lines (209-210). “. . when the ANP is greater than 2 (that is the amplitude greater than 8 cm) . .” These two criteria are not the same thing. It is possible for ANP < 2 but amplitude > 8 cm for a large eddy.

Ans: Thank you. The sentence has been revised in the revised version (P12, line 226). We fully agree with you. But, as our research shown, the ANP > 2 and the amplitude > 8cm is corresponding. As for the existence of the phenomenon you mentioned, more researches are needed to verify it and we will strengthen this research in subsequent investigation.

Line 210. “well reproduced”. Referee 1 main comment 3 asks for an objective measure for good reproduction. Please say how you measure it.

Ans: Thank you. In this study, we can only be qualitative, cannot quantitatively determine the quality of reproduction. As for the criterion, we mainly judge whether the eddy center distance and the amplitude change trend are consistent between the observed and the assimilation results.

Line 218. “. . CSCASS: the meridional and zonal radii of AE1 . .”

Ans: Thank you. The sentence has been revised in the revised version. (P12, line 235)

Lines 223-224. “. . (Fig. 7b-7j), e.g. moving northwestward firstly and then southwestward, can generally . .”

Ans: Thank you. The sentence has been revised in the revised version. (P12, line 240-241)

Page 12.

Line 230. “. . their observed amplitude”

Ans: Thank you. The sentence has been revised in the revised version. (P13, line 248-249)

Line 232. “relatively small, less than 8 cm, . .”. But this criterion “8 cm” may depend on altimeter accuracy (Referee 1 main comment 2). You should discuss how the criterion might differ in other contexts. Most readers will not be repeating your work in the NSCS but may want to know a criterion in their context.

Ans: Thank you. The sentence has been revised in the revised version (P13, line 249). Yes, the criterion “8 cm” is relating with the SLA error of assimilation system. For

example, the mean SLA error of the CSCASS in the SCS is about 8cm.

Line 235. “assimilated . .”

Ans: Thank you. The word “assimilating” has been changed to “assimilated” in the revised version. (P13, line 252)

Page 13.

Line 253. “2004 . .”

Ans: Thank you. The year “2003” has been changed to “2004” in the revised version. (P14, line 270)

Line 255. “disappearance”

Ans: Thank you. The word “disappear” has been changed to “disappearance” in the revised version. (P14, line 272)

Page 14.

Line 273. “. . and then enhancement of AE1 was also predicted . .”

Ans: Thank you. The sentence has been revised in the revised version. (P14, line 290)

Line 278. Delete “which”.

Ans: Thank you. The word “which” has been deleted in the revised version. (P15, line 295)

Line 279. “continued”

Ans: Thank you. The word “continue” has been changed to “continued” in the revised version. (P15, line 296)

Line 284. “reproduce . .”

Ans: Thank you. The word “reproduced” has been changed to “reproduce” in the revised version. (P15, line 300)

Line 287. “. . but the predicted movement is firstly toward . .”

Ans: Thank you. The sentence has been revised in the revised version. (P15, line 304)

Page 15.

Line 296. “slow”

Ans: Thank you. The word “slowly” has been changed to “slow” in the revised version. (P15, line 313)

Line 309. “. . and movement direction . .”

Ans: Thank you. The word “moving” has been changed to “movement” in the revised version. (P16, line 325)

Lines 310-311. “. . AE2 are keeping in the consistent trend (Fig. 14e), . .”. This is very unclear. Also the figure does not show much consistency between the observed amplitude (overall decrease) and predicted amplitude (overall increase), but the observed and predicted amplitudes are getting closer with time.

Ans: Thank you. The sentence has been revised in the revised version. (P16, line 327-328)

Page 16.

Line 316. “owing to the low amplitude . .”

Ans: Thank you. The sentence has been revised in the revised version. (P16, line 333)

Line 325. “. . production and predictability . .”

Ans: Thank you. The word “productivity” has been changed to “production” in the revised version. (P17, line 342)

Lines 327-328. Better “. . The comparisons of AE1 and AE2 observations with CSCASS prediction experiments, which assimilate SLA and SST, show that . .” ?

Ans: Thank you. The sentence has been revised in the revised version. (P17, line 344-345)

Line 331. “disappearance”. Again there is the question of what uncertainty determines the value 8 cm.

Ans: Thank you. As our result shows, the SLA error of assimilation system determines the value 8 cm.

Lines 333-334. “. . prediction experiments . . with observations . .”

Ans: Thank you. The sentence has been revised in the revised version. (P17, line 350-351)

Page 17.

Line 336. “generation”

Ans: Thank you. The word “generative” has been changed to “generation” in the revised version. (P17, line 353)

Lines 341-342. “. . reproduction and predictability. As . .”

Ans: Thank you. The sentence has been revised in the revised version. (P18, line 358)

Lines 348-350. Better “it cannot make up for limitations of numerical model algorithms and resolution. Hence for high-resolution operational oceanography, numerical models ..”

Ans: Thank you. The sentences have been revised in the revised version. (P18, line 364-366)

Page 20 lines 404-407. These two references should be in reversed order.

Ans: Thank you. The order of the two references has been corrected in the revised version. (P21, line 421-424)

1 **Could the two anticyclonic eddies during winter 2003/2004 be reproduced and**
2 **predicted in the northern south China sea?**

3

4 Dazhi Xu ^{1,3}, Wei Zhuang⁴, Youfang Yan ^{2*}

5

6 ¹South China Sea Marine Prediction Center, State Oceanic Administration, Guangzhou, China

7 ²South China Sea Institute of Oceanology, Chinese Academic of Science, Guangzhou, China

8 ³Nansen Environmental and Remote Sensing Center, Bergen, Norway

9 ⁴State Key Laboratory of Marine Environmental Science & College of Ocean and Earth

10 Sciences, Xiamen University, Xiamen 361102, China

11

Abstract

12 Great progress has been made in understanding the mesoscale eddies and their role on
13 the large-scale structure and circulation of the oceans. However, many questions still
14 remain to be resolved, especially with regard to the reproductivity and predictability of
15 mesoscale eddies. In this study, the reproductivity and predictability of mesoscale
16 eddies in the Northern SCS (NSCS), a region with strong eddy activity, are investigated
17 with a focus on two typical anticyclonic eddies (AE1 and AE2) based on a HYCOM-
18 EnOI Assimilated System. The comparisons of assimilated results and observations
19 suggest that generation, evolution and propagation paths of AE1 and AE2 can be well
20 reproduced and forecasted when the observed amplitude >8 cm (or the advective
21 nonlinearity parameter U/c greater than 2), although their forcing mechanisms are quite
22 different. However, when their amplitudes are less than 8 cm, the generation and decay
23 of these two mesoscale eddies cannot be well reproduced and predicted by the system.
24 This result suggests, in addition to dynamical mechanisms, the spatial resolution of
25 assimilation observation data and numerical models must be taken into account in
26 reproducing and predicting mesoscale eddies in the NSCS.

27

28 **Keywords:** HYCOM; EnOI; Northern South China Sea; Mesoscale eddy;
29 Predictability

30 1. Introduction

31 Equivalent to the synoptic variability of the atmosphere, ~~the~~ ocean mesoscale
32 eddies ~~is~~ are often described as the “weather” of the ocean, with typical spatial scales
33 of ~100 km and time scales of a month (Wang et al., 1996; Liu et al., 2001; Chelton et
34 al., 2011). The mesoscale eddy is characterized by temperature and salinity anomalies
35 with associated flow anomalies, exhibiting different properties to their surroundings,
36 thus allowing them to control the strength of mean currents and to transport heat, salt,
37 and biogeochemical tracers around the ocean. The motion of mesoscale eddies would
38 be a straight line, if eddies freely propagate in open ocean. However, most of eddies
39 may have interaction with topography, strong currents (western boundary current),
40 eddies during their lifetime. The motion of eddy will be modified and even split when
41 approaching an island (Yang et al., 2017). It is also recognized that western boundary
42 is graveyard of eddies (Zhai et al., 2010). The dynamical processes such as splitting
43 and/or merging of eddies can also make termination and/or genesis of eddies in open
44 ocean (Li et al., 2016). Thus, the dynamical processes make that the prediction of eddy
45 motion is a challenge for ocean simulation. Although today, the beauty and complexity,
46 the scales resolved, the eddy energy and tracking and the effects on atmosphere of these
47 mesoscale features can be seen by viewing high resolution satellite images or numerical
48 model simulations (Yang et al., 2000; Fu et al., 2010; Morrow and Le Traon, 2012;
49 Frenger et al., 2013), the operational forecasts of the mesoscale eddy still pose a big
50 challenge because of its complicated dynamical mechanisms and high nonlinearity
51 (Woodham et al., 2015; Treguier et al., 2017; Vos et al., 2018). A recent example is the

52 explosion of the Deepwater Horizon drilling platform in the northern Gulf of Mexico
53 in 2010 where an accurate prediction of the position and propagation of the Loop
54 Current eddy was essential in determining if the spilled oil would be advected to the
55 Atlantic Ocean or still remain within the Gulf (Treguier et al., 2017).

56 Similar to Gulf of Mexico, the South China Sea (SCS) is also a large semi-closed
57 marginal sea in the northwest Pacific, connecting to the western Pacific through the
58 Luzon Strait (Fig. 1). Forced by seasonal monsoon winds, the intrusion of Kuroshio
59 Current (KC), the Rossby waves and the complex topography, the SCS, especially the
60 Northern SCS (NSCS) exhibits ~~a significantly high~~ mesoscale eddy activity (Fig. 2).
61 Many studies have tried to investigate ~~the mesoscale eddy eddies~~ in the NSCS (Wang
62 et al., 2003; Jia et al., 2005; Wang et al., 2008). Based on the potential vorticity
63 conservation equation and in-situ survey data, Yuan and Wang (1986) pointed out that
64 the bottom topography forcing might be the primary factor for the formation of
65 anticyclonic eddies in the northeast of Dongsha Islands (DIs). Using survey CTD data
66 in September 1994, Li et al (1998) recorded ~~the evidence~~ of anticyclonic eddies in the
67 NSCS and suggested these anticyclonic eddies are probably shed from the KC.
68 Investigations by Wu et al. (2007) showed that westward propagating eddies in the
69 NSCS originate near the Luzon Strait rather than coming from the western Pacific.
70 Based on the altimeter, the trajectory of drift and the hydrological observations data,
71 Wang et al. (2008) studied the evolution and migration of two anticyclonic eddies in
72 the NSCS during winter of 2003/2004. As they described, the AE1 generated by
73 interaction of the unstable rotating fluid with the sharp topography of DIs firstly

74 appeared near DIs on the 10th of December 2003 (see Fig. 3). Then it began to move
75 southwestward with its amplitude decreasing gradually. During the movement of AE1,
76 another anticyclonic eddy (AE2) was shed and developed from the loop current of
77 Kuroshio near the Luzon Strait on the 14th of January 2004. The amplitude of AE2 was
78 then increased when it propagated southwestward (Fig. 3d-3f). About five weeks later,
79 AE2 reached its maximum in amplitude and then lasted around three weeks in its
80 mature state. During its decay phase, AE2 moved southwestward quickly with its
81 amplitude decreasing, and finally disappeared at the location of 114°E, 18°N on the 7th
82 of April 2004. ~~In the m~~Meanwhile, AE1 continued moving to southwest and eventually
83 disappeared ~~in the southeastern~~ of Hainan. In addition to physical characteristics, the
84 phytoplankton community at these two eddies have also been studied by Huang et al.
85 (2010). These studies improved our understanding of activities of mesoscale eddy and
86 its possible dynamical mechanisms in the NSCS.

87 Despite ~~the studies on~~ the activities and its possible dynamical mechanisms of
88 mesoscale eddies in the NSCS ~~have~~ having received much attention in past decades,
89 studies on the reproductivity and predictability of mesoscale eddies in the NSCS are
90 still rare. As mentioned above, mesoscale eddies are not only related to complicated
91 dynamical mechanisms but also involve strong nonlinear processes (Oey et al, 2005);
92 ~~thus~~ they are not a deterministic response to atmospheric forcing. The quality of
93 mesoscale eddies forecasting will depend primarily on the quality of the initial
94 conditions. Ocean data assimilation, which combines observations with the numerical
95 model, can provide more realistic initial conditions and thus is essential for the

96 prediction of mesoscale eddies. As shown by previous studies, after assimilating
97 altimeter data into ocean models, the ocean currents in the southern SCS (Xiao et al.,
98 2006) and the realism of three largest eddies in the SCS appear during Typhoon
99 Rammasun (Xie et al., 2018) have been improved. Furthermore, some studies show that
100 the ocean model includes tides or assimilated altimeter data with reasonable MDT, can
101 provide more realistic initial conditions (Xie et al., 2011; Xu et al., 2012). The above
102 studies show that the mesoscale eddies in the SCS are reproducible, but about the
103 predictability of mesoscale eddies is rare. In this study, we assessed the reproduction
104 and predictability of two typical anticyclonic eddies (Wang et al., 2008), owing to be
105 represented different generation mechanisms and survive long enough to be useful, in
106 the NSCS with focus on their generation, evolution and decay processes by a series of
107 numerical experiments based on a Chinese Shelf/Coastal Seas Assimilation System
108 (CSCASS; Li, 2009; Li et al., 2010; Zhu, 2011) along with the observation data from
109 surface drifter trajectory and satellite remote sensing.

110 **2. Datasets and Methodologies**

111 **2.1 Datasets**

112 In this study, the altimetric data between 2003-2004, which includes along-track
113 SLA, totally 29 passes (about 9300 points) over the domain of CSCS was selected.
114 Considering the noise of SLA measurement in the shallow seas, data for the shallow
115 areas with depth<400 m was excluded. In order to verify, the merged SLA based on
116 Jason-1, TOPEX/Poseidon, ERS-2 and ENVISAT (Ducet et al., 2000) provided by

117 Archiving, Validation and Interpretation of Satellites Oceanographic data (AVISO) at
118 Centre Localization Satellite (CLS, <ftp://ftp.aviso.oceanobs.com/global/nrt/>) with $1/4^\circ$
119 $\times 1/4^\circ$ resolution and weekly average are used. In addition, because the SLA present
120 only the anomalies relative to a time-mean sea level field, thus a new mean dynamic
121 topography (nMDT), which has been corrected using iterative method by Xu et al.
122 (2012) was used to calculate the realistic sea level in this study.

123 In addition to SLA datasets, the daily OISST from the National Oceanic and
124 Atmospheric Administration's (NOAA) National Climatic Data Center
125 (<ftp://eclipse.ncdc.noaa.gov/pub/OI-daily-v2/NetCDF/>), which was merged by an
126 optimum interpolation method (Reynolds et al., 2007) based on the Infrared SST
127 collected by the Advanced Very High Resolution Radiometer sensors on the NOAA
128 Polar Orbiting Environmental Satellite and SST from Advanced Microwave Scanning
129 Radiometer for the Earth Observing System, are also used. The daily OISST's biases
130 were fixed using in situ data from ships and buoys. The dataset between 2003 and 2004
131 was used in this study, with a spatial resolution of $1/4^\circ \times 1/4^\circ$. In addition, the surface
132 drifting buoy data from the World Ocean Circulation Experiment (WOCE,
133 <ftp://ftp.aoml.noaa.gov/pub/phod/buoydata/>) are also used. ~~A total of 3~~ Three drifters
134 were designed to drift at the surface within the upper 15 m and tracked by the ARGOS
135 satellite system. Positions of the drifters were smoothed using a Gaussian-filter scale of
136 24 h to eliminate tidal and inertial currents, and were subsampled at 6 h intervals
137 (Hamilton et al, 1999).

138 **2.2 Method of identify the mesoscale eddies**

139 Similar to the standard of Cheng et al (2005) and Chelton et al (2011), we identify
140 the mesoscale eddies in this study ~~is~~ as follows: 1) there must be a ~~closed~~ closed contour
141 on the merged SLA; 2) there must ~~have-be~~ have-be one maximum or minimum inside the area
142 of ~~the closedure~~ the closedure contour for anticyclonic or cyclonic eddy; 3) the difference between
143 the extremum and the outermost ~~closedure of SLA contour~~ closedure of SLA contour, that is, the amplitude of the
144 mesoscale eddy, must be greater than 2 cm; and 4) the spatial scale of the eddy should
145 be 45-500 km. In addition, the amplitude (A) of an eddy is defined here to be the
146 magnitude of the difference between the estimated basal height of the eddy boundary
147 and the extremum value of SSH within the eddy interior: $A=|h_{ext}-h_0|$.

148 2.3 Ocean model

149 We here used a three-dimensional hybrid coordinate ocean model (HYCOM;
150 Halliwell et al, 1998; 2000; Bleck, 2002; Halliwell, 2004; Chassignet et al, 2007) to
151 provide a dynamical interpolator of observation data in the assimilation system.
152 HYCOM is a primitive equation general ocean circulation model with vertical
153 coordinates: isopycnic coordinate in the open stratified ocean, the geopotential (or z)
154 coordinate in the weakly stratified upper ocean, and the terrain following sigma-
155 coordinate in shallow coastal regions.

156 In this study, HYCOM was implemented in the Chinese shelf/coastal seas with a
157 horizontal resolution of $1/12^\circ \times 1/12^\circ$, and in the remaining regions with $1/8^\circ \times 1/8^\circ$, the
158 model domain is from 0°N to 53°N and from 99°E to 143°E , the detail model domain
159 and grid can refer to the inset panel of Fig.1. The vertical water column from the sea
160 surface to the bottom was divided into 22 levels. The K-Profile Parameterization (KPP;

161 Large et al., 1994), which has proved to be an efficient mixing parameterization in many
162 oceanic circulation models, was used here. The bathymetry data of the model domain
163 were taken from the 2-Minute Gridded Global Relief Data (ETOPO2).

164 To adjust the model dynamics and achieve a perpetually repeating seasonal cycle
165 before applying the interannual atmospheric forcing, the model was initialized with
166 climatological temperature and salinity from the World Ocean Atlas 2001 (WOA01;
167 Boyer et al., 2005) and was driven by the Comprehensive Ocean-Atmosphere Data Set
168 (COADS; Woodruff et al., 1987) in the spin-up stage. After integrating ten model years
169 with climatological forcing, the model was forced by the European Center for Medium-
170 Range Weather Forecasts (ECMWF) 6-hourly reanalysis dataset (Uppala et al., 2005)
171 from 1997 to 2003. The wind velocity (10-m) components were converted to stresses
172 using a stability dependent drag coefficient from Kara et al. (2002). Thermal forcing
173 included air temperature, relative humidity and radiation (shortwave and longwave)
174 fluxes. Precipitation was also used as a surface forcing from Legates ~~and Wilmott et al.~~
175 (1990). Surface latent and sensible heat fluxes were calculated using bulk formulae
176 (Han, 1984). Monthly river runoff was parameterized as a surface precipitation flux in
177 the ECS, the SCS and Luzon Strait (LS) from the river discharge stations of the Global
178 Runoff Data Centre (GRDC) (<http://www.bafg.de>), and scaled as in Dai et al. (2002).
179 Temperature, salinity and currents at the open boundaries were provided by an India-
180 Pacific domain HYCOM simulation at $1/4^\circ \times 1/4^\circ$ spatial resolution (Yan et al., 2007).
181 Surface temperature and salinity were relaxed to climate on a time scale of 100 days.
182 Both two-dimensional barotropic fields such as Sea Surface Height and barotropic

183 velocities, and three-dimensional baroclinic fields such as currents, temperature,
 184 salinity and density were stored daily.

185 2.4 The assimilation scheme

186 The ensemble optimal interpolation scheme (EnOI; Oke et al., 2002), which is
 187 regarded as a simplified implementation of the Ensemble Kalman Filter (EnKF), aims
 188 at alleviating the computational burden of the EnKF by using stationary ensembles to
 189 propagate the observed information to the model space. The data assimilation schemes
 190 can be briefly written as (Oke et al., 2010):

$$191 \quad \vec{\psi}^a = \vec{\psi}^b + K(\vec{d} - H\vec{\psi}^b) \quad (1)$$

$$192 \quad K = P^b H^T [H P^b H^T + R]^{-1} \quad (2)$$

193 where $\vec{\psi}$ is the model state vectors including model temperature, layer thickness and
 194 velocity; Superscripts a and b denote analysis and background, respectively; \vec{d} is
 195 the measurement vector that consists of SST and SLA observations; K is the gain
 196 matrix; and H is the measurement operator that transforms the model state to
 197 observation space. P is the background error covariance and R is the measurement
 198 error covariance. In EnOI, Eq. 2 can be expressed as:

$$199 \quad K = \alpha(\sigma \circ P^b) H^T [\alpha H(\sigma \circ P^b) H^T + R]^{-1} \quad (3)$$

200 where α is a scalar that can tune the magnitude of the analysis increment; σ is a
 201 correlation function for localization; and P^b is the background error covariance which
 202 can be estimated by

$$203 \quad P^b = A' A'^T / (n - 1) \quad (4)$$

204 In Eq. 4, n is the ensemble size, A' is the anomaly of the ensemble matrix, $A =$
205 $(\psi_1, \psi_2, \dots, \psi_N) \in \mathfrak{R}^{n \times N}$ ($\psi_i \in \mathfrak{R}^N (i = 1, \dots, n)$) is the ensemble members, N is the
206 dimension of the model state, representing usually the model variability at certain scales
207 by using a long-term model run or spin-up run. More detailed description and
208 evaluation of the CSCASS are in Li et al. (2010) and Xu et al. (2012).

209

210 3. Results

211 3.1 The reproduction of ~~these~~ anticyclonic eddies AE1 and AE2 in the NSCS

212 In order to investigate whether the evolution and migration features of these two
213 eddies can be reproduced by the CSCASS or not, we firstly set up an assimilation
214 experiment named As_exp (see Fig. 4, black line) for AE1 and AE2. In this experiment,
215 the observed SST and SLA are both assimilated into CSCASS ~~at an equal interval of~~
216 every 3 days. To meet dynamic adjustment, the first assimilation was performed on the
217 27th of September 2003, two months prior to the generation of AE1.

218 Base on the As_exp experiment output, we use the observations SLA to evaluate
219 the uncertainty of CSCASS in the research area. In this study, we calculated the weekly
220 mean RMS error (RMSE) of the As_exp /control experiments output and observations
221 for SLA. As the result indicates, the RMSE for the As_exp is between 6 cm to 14 cm,
222 while RMSE for the control is between 10 cm to 18 cm. This result suggested that data
223 assimilation improved effectively the SLA field and had a beneficial impact on model
224 results in this area.

225 In addition, we also use the Advective Nonlinearity Parameter U/c (ANP, Chelton

226 et al., 2011; Li et al., 2014; 2015; 2016; Wang et al., 2015) as a criterion to estimate the
227 eddy forecast ability of the CSCASS. As fig. 5 shows, when the ANP is greater than 2
228 (that is the amplitude greater than 8 cm) AE2 can be well reproduced by the CSCASS.

229 Besides, we also use the independent evaluation, Fig.6 compared the assimilating
230 results of AE1 with the observations both from the satellite remote sensing and drifter
231 buoys trajectories of number 22517, 22918 and 22610 between December 3rd 2003 and
232 February 18th 2004. From Fig. 6 and Table 1, we can see that the generation and
233 movement of AE1 can be well reproduced by the CSCASS, with the pink curves
234 (assimilation) match well with those of black (satellite observations) and dotted lines
235 (the trajectories of drifter buoys). In addition, the spatial pattern of AE1 can also be well
236 revealed by the CSCASS: the ~~radius of~~ meridional and zonal radii of AE1 detected by
237 the assimilation are 163 km and 93 km, which are almost equal to that of observations
238 (148 km and 79 km). The migration path of AE1 can also be well reproduced by the
239 CSCASS (see Fig. 6, black and pink line) until its amplitude decays to less than 8 cm.
240 In addition to AE1, the generation and evolution of AE2 are also evaluated. As shown
241 Fig. 7, the evolution and propagation pathway of AE2 (Fig. 7b-7j), e.g., ~~move~~ moving
242 northwestward firstly and then southwestward, can generally be reproduced by the
243 CSCASS, although its initial location shows a slight southward bias in the simulation
244 (Fig. 7a). Similar to the results of AE1, discrepancies between model and observations
245 become larger again during the decay phase of AE2.

246 In general, the comparison of assimilation SLA with that of satellite observation
247 and the trajectories of drifter buoys suggested that the generation, development and the

248 propagation of AE1 and AE2 can be reproduced by the CSCASS when their observed
249 amplitude greater than 8 cm (or the ANP greater than 2). However, when their
250 amplitudes are relatively small, ~~with values~~ less than 8 cm, the features of these two
251 mesoscale eddies are not well reproduced by the CSCASS. This may be related to the
252 value setting of parameter α , the localization length scale, and insufficient spatial
253 resolution of ~~assimilating~~ assimilated SSH or the numerical model (Counillon and
254 Bertino, 2009).

255 3.2 The predictability of these anticyclonic eddies in the NSCS

256 Since the generation, development and the propagation of AE1 and AE2 can be
257 well reproduced by the CSCASS when their amplitude > 8 cm (or the ANP greater than
258 2), as mentioned above, in this section we further use the CSCASS to investigate the
259 predictability of these two eddies. According to the generation, evolution and migration
260 of these two eddies, we designed six forecast experiments, hereafter referred to as Exp1
261 to Exp6 (see Fig.4) to investigate their predictability. The model's initial state prior to
262 each of the six forecast experiments is constrained by assimilating satellite SLA and
263 SST before. Based on the initial state, each experiment is run forward 30 days with the
264 forcing of 6-hourly wind, surface heat flux, and monthly mean river runoff, etc. The
265 first experiment, named Exp1, is applied on the 29th of November 2003, which tends to
266 study whether the generation of AE1 can be forecasted or not. Exp2 is implemented on
267 the 10th of December 2003 and is used to study whether the development and the
268 migration of AE1 can be forecasted. Exp3 is run based on the initial state on the 31th of
269 December 2003 and used to show whether the generation of AE2 and the continued

270 migration of AE1 can be forecasted. In order to investigate whether the continued
271 evolution of AE1 and AE2 can be forecasted, Exp4 is applied on the 21th of January
272 ~~2003~~2004. Exp5, is setting up to reveal whether the attenuation of AE1 and the
273 evolution of AE2 can be forecasted, while Exp6 which is applied on the 29th of February
274 2004 was designed to find out whether the disappearance of AE1 and AE2 can be
275 forecasted.

276 The prediction results of Exp1 are shown in Fig. 8. In Fig. 8a, we can see that the
277 forecast is almost coincident with the satellite observation and the trajectory of drift
278 buoys, indicating that the generated position of AE1 can be well forecasted by the
279 CSCASS. In addition, the initial migration of AE1 can also be forecasted by the
280 CSCASS (see Fig. 8a and 8f). In order to evaluate the forecasted amplitude of AE1, the
281 amplitude and the distance of eddy centers between the observation and the forecast are
282 also quantified (Table 2: EXP1). From Table 2: EXP1, we can see that the amplitude of
283 forecasting matches well with that of observation, although its amplitude is slightly
284 larger than that of observation. After 4 weeks, the amplitude of the forecast is still close
285 to those of the observation, suggesting that the generation of AE1 can be well predicted
286 by the CSCASS.

287 In order to find out whether the development and movement path of AE1 can be
288 predicted after generation, we continue to carry out Exp2. As shown by the observation
289 (Fig. 9), AE1 moves southwestward along the continental shelf with its amplitude
290 decreasing and again increasing after its generation. This observed southwestward
291 movement is also predicted by the CSCASS (see pink closure curve in Fig. 9a-9d),

292 although a sudden southwestward movement cannot be well predicted (Fig. 9f). In
293 addition, the first attenuation and then ~~enhancement~~~~enhance~~ of AE1 can also been
294 predicted by the CSCASS (see Table 2 and Fig. 9b). On the whole, the development
295 and movement path of AE1 can be well predicted by CSCASS for the first four weeks
296 after its generation. After that, the errors between observation and prediction increase
297 significantly, and by the fifth week, the distance between the center of the prediction
298 and the observation become larger, ~~which~~ more than 100 km (see Fig. 9e).

299 For further analysis, we carry out Exp3, to look at whether the continued evolution
300 of AE1 and the generation of AE2 can be predicted. This experiment is carried out based
301 on the initial condition of the assimilation on the 31st of December 2003 and the
302 corresponding results are shown in Fig. 10 and Table 2. As shown by the prediction
303 (Fig. 10, Table 2), although with a slightly weak amplitude, the CSCASS can
304 reproduce AE1 after assimilating SLA and SST and predicted its development trend.
305 In addition, the movement path of AE1 cannot be accurately predicted at this period,
306 for instance, the observed AE1 moves directly to southwest (see red solid line and solid
307 circle in Fig. 10f), but the ~~prediction's predicted~~ movement is firstly toward northeast,
308 then turns to southwest (see blue solid line and solid circle in Fig. 10f). The generation
309 of AE2 cannot be predicted in Exp3, which may be related to the smaller amplitude (<8
310 cm) of AE2 at this period.

311 The purpose of Exp4 is to look at whether the evolution of AE1 and AE2 can both
312 be reasonably predicted. Since this experiment mainly focuses on the evolution of AE1
313 and AE2, thus Fig. 11 shows only the evolution of AE2 from the second week after

314 generation, that is, from the beginning on the 21st of January 2004 to the fifth week. As
315 shown in Fig. 11, Table 2 and Fig. 14d, the trends of amplitude variation of both eddies
316 can be well predicted with the decreasing of AE1 and slowly increasing of AE2. For
317 AE1, the results of the prediction and observation are very close in the first two weeks,
318 with the center of the two almost coincide. The central position of the prediction and
319 observation began to deviate after the third week. For AE2, although the amplitude and
320 movement path are not predicted well at its initial stage, the prediction is slowly
321 approaching to the observation during third to fifth week, and distance between the
322 center of the prediction and the observation is reduced from 132 km at the beginning to
323 81 km at the end (see Fig. 14d the black solid line).

324 As mentioned above, the purpose of Exp5 is to investigate whether the decay of
325 AE1 and the continued development of AE2 can be predicted. From Fig. 12, Table 2
326 and Fig. 14e, we can find that the CSCASS cannot predict the movement path of AE1
327 well in its decay stage: the distance between the center of the prediction and that of the
328 observation is greater than 188 km, and ~~the moving movement~~ direction of the two is
329 not consistent (see red lines and dots in Fig. 12f). But the evolution and moving
330 direction of AE2 can be well predicted at this stage. The amplitude of observation and
331 prediction of AE2 are ~~getting closer with timekeeping in the consistent trend~~ (Fig. 14e),
332 although the speed of movement of AE2 given by prediction is slower than that of
333 observation (see blue dashed lines and hollow dots in Fig. 12f).

334 The aim of Exp6 is to find whether the disappearance of AE1 and AE2 can be both
335 predicted. As described in Fig. 13, the disappearance of AE1 cannot be well predicted

336 ~~since-owing to~~ the low amplitude (less than 8 cm) of AE1 at this stage. Similarly, the
337 disappearance of AE2 is also less accurately predicted by the CSCASS (Fig. 14f). The
338 amplitude of AE2 from the observation decays continually at this stage, but the
339 amplitude of the predicted almost keeps constant. In addition, there is large deviation
340 of the direction of movement between prediction and observation for AE2 (see the red
341 solid line and dot in Fig. 13f).

342

343 4. Conclusions and challenges for forecasting of mesoscale eddy

344 In this paper, we carry out a series of assimilation and prediction experiments by
345 the CSCASS to assess the ~~productivity-production~~ and predictability of mesoscale
346 eddies in the NSCS, along with observations of satellite observed SST, SLA and the
347 trajectory data of drift. The comparisons of AE1 and AE2 ~~observations withby the~~
348 CSCASS ~~prediction experiments~~, which ~~is assimilated~~ SLA and SST, ~~with that of~~
349 ~~observations through predicted experiments~~ shows that when the amplitudes of
350 mesoscale eddy are higher than 8 cm, the generation, development, decay and
351 movement of eddies can be well reproduced, but when the amplitude of the mesoscale
352 eddy is lower than 8 cm, the generation and ~~disappearance~~ of mesoscale eddy cannot
353 be well reproduced.

354 The comparisons of AE1 and AE2 through six ~~predicted-prediction~~ experiments
355 with ~~those of~~ observations also show that the generation, evolution and movement path
356 of these two eddies with high amplitude (>8 cm or the ANP greater than 2) can be well
357 predicted by the CSCASS, although the ~~generationgenerative~~ mechanism of these two

358 eddies is quite different (Wang et al., 2008). However, when the amplitude of eddies
359 becomes less than 8 cm, the generation position and the movement path cannot be well
360 predicted by the CSCASS.

361 Our results suggested that for powerful mesoscale eddies, a good initial condition
362 after assimilating observations can help to improve their [reproduction and](#)
363 [predictability](#)~~reproduced and predictable ability~~. As mentioned above, the mesoscale
364 eddies are related to strong nonlinear processes and are not a deterministic response to
365 atmospheric forcing, thus the quality of mesoscale eddies forecast will depend primarily
366 on the quality of the initial conditions. In addition, the ability of the ocean numerical
367 model to faithfully represent the ocean physics and dynamics is also crucial. Although
368 data assimilation, which combines observations with the numerical model, can provide
369 good initial conditions, it cannot make up ~~for the~~ limitations of numerical model ~~in~~
370 ~~numerical~~ algorithms and in its resolution. ~~Hence F~~for a high-resolution operational
371 oceanography, ~~the latter means that the~~ numerical models need to be improved using
372 more accurate numerical algorithms and resolution especially in the weakly stratified
373 regions or on the continental shelf.

374 Furthermore, so far most of the information about the ocean variability is obtained
375 remotely from satellites (SSH and SST), the information about the subsurface
376 variability are very rare. Although a substantial source of subsurface data is provided
377 by the vertical profiles (i.e., expendable bathy thermographs, conductivity temperature
378 depth, and Argo floats), the datasets are still not sufficient to determine the state of the
379 ocean. In addition, in order to accurately assimilate the SSH anomalies from satellite

380 altimeter data into the numerical model, it is necessary to know the oceanic mean SSH
381 over the time period of the altimeter observations (Xu et al., 2011; Rio et al., 2014).
382 This is also a big challenge because the earth's geoid is not presented with sufficient
383 spatial resolution when assimilating SSH in an eddy-resolving model. With the advent
384 of the SWOT (Surface Water and Ocean Topography) satellite mission in 2020, it
385 should be possible to better resolve and forecast the mesoscale features in eddy
386 resolving ocean forecasting systems.

387

388 **Acknowledgements:**

389 This study is supported by the Marine Science and Technology Foundation of South
390 China Sea Branch, State Oceanic Administration (grant 1447), the National Key
391 Research and Development Program of China (2016YFC1401407), the Project of
392 Global Change and Air-Sea interaction under contract No. GASI-03-IPOVAI-04, the
393 National Natural Science Foundation of China (Grant No. 41731173, 41776037 and
394 41276027), and the China Scholarship Council (award to Xu Dazhi for 1 year's study
395 abroad at Nansen Environmental and Remote Sensing Center).

396

397 **References:**

- 398 Bleck, R.: An oceanic general circulation model framed in hybrid isopycnic cartesian
399 coordinates, *Ocean Model*, 4, 55-88, 2002.
- 400 Boyer, T. P., Levitus, S., Antonov, J. I., et al.: Linear trends in salinity for the World Ocean,
401 1955-1998, *Geophys. Res. Lett.*, 32, 67-106, 2005.
- 402 Chassignet, E. P., Hurlburt, H. E., Smørdstad, O. M., et al.: The HYCOM (Hybrid Coordinate
403 Ocean Model) data assimilative system, *J. Mar. Sys.*, 65, 60-83, 2007.
- 404 Chelton, D. B., Schlax, M. G., and Samelson, R. M.: Global observations of nonlinear
405 mesoscale eddies, *Progr. in Oceanogr.*, 91, 167-216, 2011.
- 406 Cheng, X. H., Qi, Y. Q., and Wang, W. Q.: Seasonal and Interannual Variabilities of Mesoscale
407 Eddies in South China Sea, *J. Trop. Oceanogr.*, 24, 51-59, 2005.
- 408 Counillon, F., and Bertino, L.: Ensemble Optimal Interpolation: multivariate properties in the
409 Gulf of Mexico, *Tellus*, 61A, 296-308, 2009.
- 410 Dai, A., and Trenberth, K. E.: Estimates of freshwater discharge from continents: latitudinal
411 and seasonal variations, *J. Hydrometeorol.*, 3, 660-685, 2002.
- 412 Ducet, N., LeTraon, P. Y., and Reverdin, G.: Global high-resolution mapping of ocean
413 circulation from TOPEX/Poseidon and ERS-1 and-2, *J. Geophys. Res.*, 105, 19477-19498,
414 2000.
- 415 Frenger, I., Gruber, N., Knutti, R., and Münnich, M.: Imprint of Southern Ocean eddies on
416 winds, clouds and rainfall, *Nat. Geosci.*, 6, 608-612, 2013.
- 417 Fu, L.-L., Chelton, D. B., Traon, P.-Y. L., et al.: Eddy dynamics from satellite altimetry,
418 *Oceanogr.*, 23, 14-25, 2010.
- 419 Halliwell, J. G. R.: Evaluation of vertical coordinate and vertical mixing algorithms in the
420 Hybrid-Coordinate Ocean Model (HYCOM), *Ocean Model*, 7, 285-322, 2004.
- 421 Halliwell, J. G. R., Bleck, R., and Chassignet, E. P.: Atlantic Ocean simulations performed using
422 a new Hybrid Coordinate Ocean Model (HYCOM), EOS, Fall AGU Meeting, 1998.
- 423 Halliwell, J. G. R., Bleck, R., Chassignet, E. P., et al.: Mixed layer model validation in Atlantic
424 Ocean simulations using the Hybrid Coordinate Ocean Model (HYCOM), EOS, 80,

425 OS304, 2000.

426 [Hamilton, P., Fargion, G. S., and Biggs, D. C.: Loop Current eddy paths in the western Gulf of](#)
427 [Mexico, *J. Phys. Oceanogr.*, 29, 1180-1207, 1999.](#)

428 [Han, Y.-J.: A numerical world ocean general circulation model: Part II. A baroclinic experiment,](#)
429 [*Dyn. Atmos. Oceans*, 8, 141-172, 1984.](#)

430 Huang, B. Q., Hua, J., Xu, H. Z., et al: Phytoplankton community at warm eddies in the
431 northern South China Sea in winter 2003/2004, *Deep Sea Res. Part II*, 57, 1792-1798,
432 2010.

433 Jia, Y., Liu, Q., and Liu, W.: Primary studies of the mechanism of eddy shedding from the
434 Kuroshio bend in Luzon Strait, *J. Oceanogr.*, 61, 1017-1027, 2005.

435 Kara, A. B., Rochford, P. A., and Hurlburt H. E.: Air-sea flux estimates and the 1997-1998
436 ENSO event, *Boundary-Layer Meteorol.*, 103, 439-458, 2002.

437 Large, W. G., McWilliams, J. C., and Doney, S. C.: Oceanic vertical mixing: a review and a
438 model with a nonlocal boundary layer parameterization, *Rev. Geophys.*, 32, 363-403,
439 1994.

440 Legates, D. R., and Willmott, C. J.: Mean seasonal and spatial variability in gauge-corrected,
441 global precipitation, *Int. J. Climatol.*, 10, 111-127, 1990.

442 Li, L., Nowlin, W. D., and Su, J. L.: Anticyclonic rings from the Kuroshio in the South China
443 Sea, *Deep-Sea Res., Part I*, 45, 1469-1482, 1998.

444 Li, Q. Y., and Sun, L.: Technical Note: Watershed strategy for oceanic mesoscale eddy splitting,
445 *Ocean Sci.*, 11, 269-273, doi:10.5194/os-11-269-2015, 2015.

446 Li, Q. Y., Sun, L., and Lin, S.-F.: GEM: a dynamic tracking model for mesoscale eddies in the
447 ocean, *Ocean Sci.*, 12, 1249-1267, doi:10.5194/os-12-1249-2016, 2016.

448 Li, Q. Y., Sun, L., Liu, S.-S., et al: A new mononuclear eddy identification method with simple
449 splitting strategies, *Remote Sens. Lett.*, 5, 65-72. Doi:10.1080/2150704X.2013.872814,
450 2014.

451 Li, X. C.: Applying a new localization optimal interpolation assimilation module to assimilate
452 sea surface temperature and sea level anomaly into the Chinese Shelf/Coastal Seas model
453 and carry out hindcasted experiment, Graduate University of the Chinese Academy of
454 Sciences, China, 92 pp, 2009.

455 Li, X. C., Zhu, J., Xiao, Y. G., et al.: A Model-Based Observation Thinning Scheme for the
456 Assimilation of High-Resolution SST in the Shelf and Coastal Seas around China, *J.*
457 *Atmos. Oceanic Technol.*, 27, 1044-1058, 2010.

458 Liu, Z., Yang, H. J., and Liu, Q.: Regional dynamics of seasonal variability of sea surface height
459 in the South China Sea, *J. Phys. Oceanogr.*, 31, 272-284, 2001.

460 Morrow, R., and Traon, P.-Y. L.: Recent advances in observing mesoscale ocean dynamics with
461 satellite altimetry, *Adv. Spa. Res.*, 50, 1062-1076, 2012.

462 Oey, L. T., Ezer, T., and Lee, H. C.: Loop Current, rings and related circulation in the Gulf of
463 Mexico: a review of numerical models. In: *Circulation in the Gulf of Mexico: Observations and Models* Volume 161, American Geophysical Union, 31-56, 2005.

464 Oke, P. R., Allen, J. S., Miller, R. N., et al.: Assimilation of surface velocity data into a primitive
465 equation coastal ocean model, *J. Geophys. Res. Oceans*, 107, 5-1-5-25, 2002.

466 Oke, P. R., Brassington, G. B., Griffin, D. A., et al.: Ocean data assimilation: a case for ensemble
467 optimal interpolation, *Australian Meteorological and Oceanographic Journal*, 59, 67-76,
468 2010.

469 Reynolds, R. W., Smith, T. M., Liu, C., et al.: Daily High-Resolution Blended Analyses for Sea
470 Surface Temperature, *J. Climate*, 20, 5473-5496, 2007.

471 Rid, M. H., Mulet, S., and Picot, N.: Beyond GOCE for the ocean circulation estimate:
472 Synergetic use of altimetry, gravimetry, and in situ data provides new insight into
473 geostrophic and Ekman currents, *Geophys. Res. Lett.*, 41, 8918-8925, 2014.

474 Treguier, A. M., Chassignet, E. P., Boyer, A. L., et al.: Modeling and forecasting the "weather
475 of the ocean" at the mesoscale, *J. Mar. Res.*, 75, 301-329, 2017.

476 Uppala, S., Kallberg, P., Simmons, A. J., et al.: The ERA-40 re-analysis, *Q. J. R. Meteorol. Soc.*,
477 131, 2961-3012, 2005.

478 Vos, M. D., Backeberg, B., and Counillon, F.: Using an eddy-tracking algorithm to understand
479 the impact of assimilating altimetry data on the eddy characteristics of the Agulhas system,
480 *Ocean Dyn.*, 1-21, 2018.

481 Wang, D. X., Zhou, F. Z., and Qin Z. H.: Numerical simulation of the upper ocean circulation
482 with two-layer model, *Acta Oceanol Sin.*, 18, 30-40, 1996.

483 Wang, D., Xu, H., Lin, J., et al.: Anticyclonic eddies in the northeastern South China Sea during
484

485 winter 2003/2004, *J. Oceanogr.*, 64, 925-935, doi: 910.1007/s10872-10008-10076-10873,
486 2008.

487 Wang, G., Su, J., and Chu, P. C.: Mesoscale eddies in the South China Sea observed with
488 altimeter data, *Geophys. Res. Lett.*, 30, 2121, doi 10.1029/2003GL018532, 2003.

489 Wang, Z., Li, Q., Sun, L., Li, S., et al.: The most typical shape of oceanic mesoscale eddies
490 from global satellite sea level observations, *Front. Earth Sci.*, 9, 202-208. DOI
491 10.1007/s11707-014-0478-z, 2015.

492 Woodham, R. H., Alves, O., Brassington, G. B., et al.: Evaluation of ocean forecast performance
493 for Royal Australian Navy exercise areas in the Tasman Sea, *J. Oper. Oceanogr.*, 8, 147-
494 161, 2015.

495 Woodruff, S. D., Slutz, R. J., Jenne, R. L., et al.: A comprehensive ocean-atmosphere data set,
496 *Bull. Am. Meteorol. Soc.*, 68, 1239-1250, 1987.

497 Wu, C. R., and Chiang, T. L.: Mesoscale eddies in the northern South China Sea, *Deep-Sea*
498 *Res., Part II*, 54, 1575-1588, 2007.

499 Xiao, X. J., Wang, D. X., and Xu, J.-J.: The assimilation experiment in the southwestern South
500 China Sea in summer 2000, *Chin. Sci. Bull.*, 51, 31-37, 2006.

501 Xie, J. P., Bertino, L., Cardellach, E., et al.: An OSSE evaluation of the GNSS-R altimetry data
502 for the GEROS-ISS mission as a complement to the existing observational networks,
503 *Remote Sens. Environ.*, 209, 152-165, 2018.

504 Xie, J. P., Counillon, F., Zhu, J., et al.: An eddy resolving tidal-driven model of the South China
505 Sea assimilating along-track SLA data using the EnOI, *Ocean Sci.*, 8, 609-627, 2011.

506 Xu, D. Z., Li, X. C., Zhu, J., et al.: Evaluation of an ocean data assimilation system in the
507 marginal seas around China, with a focus on the South China Sea, *Chin. J. Oceanol.*
508 *Limnol.*, 29, 414-426, 2011.

509 Xu, D. Z., Zhu, J., Qi, Y. Q., et al.: Impact of mean dynamic topography on SLA assimilation
510 in an eddy-resolving model, *Acta Oceanol. Sin.*, 31, 11-25, 2012.

511 Yan, C. X., Zhu, J., and Zhou, G. Q.: Impacts of XBT, TAO, altimetry and ARGO observations
512 on the tropic Pacific Ocean data assimilation, *Adv. Atmos. Sci.*, 24, 383-398, 2007.

513 Yang, K., Shi, P., Wang, D. X., et al.: Numerical study about the mesoscale multi-eddy system
514 in the northern South China Sea in winter, *Acta Oceanol. Sin.*, 22, 27-34, 2000.

带格式的: 英语(美国)

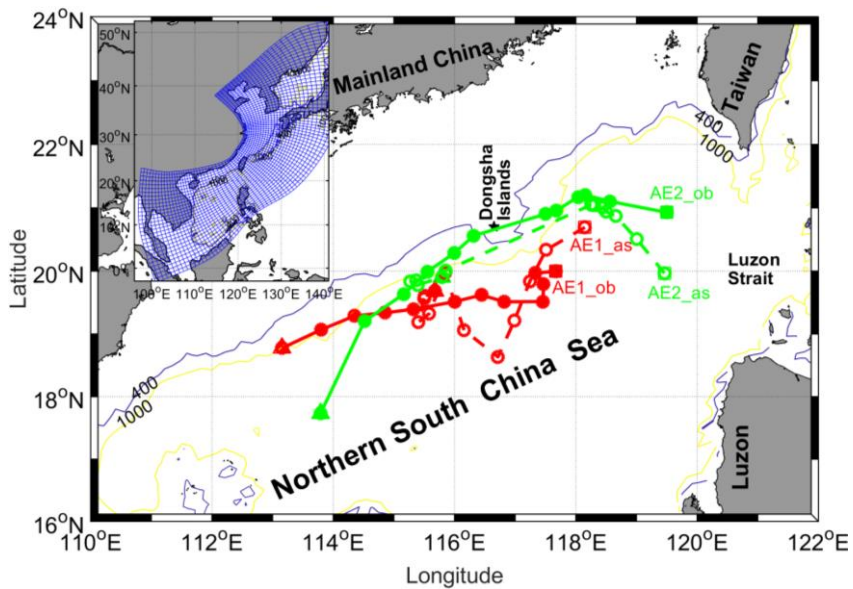
带格式的: 英语(美国)

515 Yang, S., Xing, J., Chen, D., et al.: A modelling study of eddy-splitting by an island/seamount,
516 Ocean Sci., 13, 837-849, <https://doi.org/10.5194/os-13-837-2017>, 2017.
517 Zhai X., Johnson, H. L., Marshall, D. P.: Significant sink of ocean-eddy energy near western
518 boundaries. Nat. Geosci., 3, 608-612, 2010.
519 Zhu, J.: Overview of Regional and Coastal Systems, Chapter 17 in Operational Oceanography
520 in the 21st Century. Edited by A. Schiller and G. B. Brassington, PP. 727, Springer Science,
521 Business Media B.V, 2011.
522 Zhuang, W., Du, Y., Wang, D. X., et al.: Pathways of mesoscale variability in the South China
523 Sea, Chin. J. Oceanol Limnol, 28, 1055-1067, 2010.

524

525 **Figures:**

526

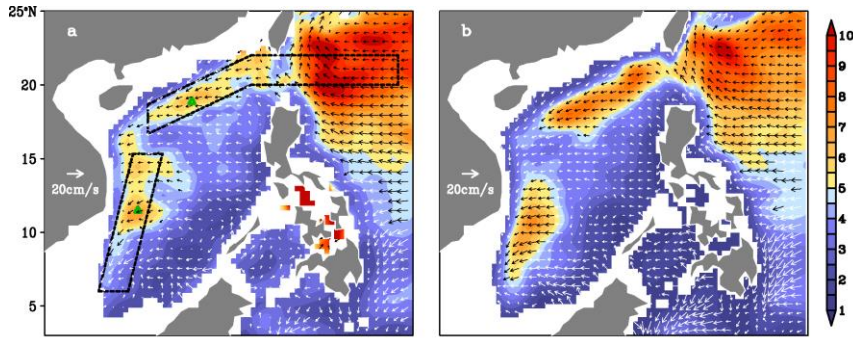


527

528 Fig. 1 Bathymetry of the northern South China Sea. The blue and yellow contour lines are the
529 isolines of 400 m and 1000 m. The solid black pentagon indicated Dongsha Islands. The migration
530 path of AE1 and AE2 in the NSCS during December 2003~April 2004. Red solid (hollow) circle
531 dots and solid (dash) lines indicated weekly passing position and migration path of observation
532 (assimilation) AE1. Green solid (hollow) circle dots and solid (dash) lines indicated weekly passing
533 position and migration path of observation (assimilation) AE2. The quadrangle and triangle denoted
534 start and end position, respectively. The model domain of CSCSS (the inset panel), the curvilinear
535 orthogonal model grid with 1/8-1/12° horizontal resolution (147×430) is denoted by the blue grid
536 (at intervals of 10 grid cells here).

537

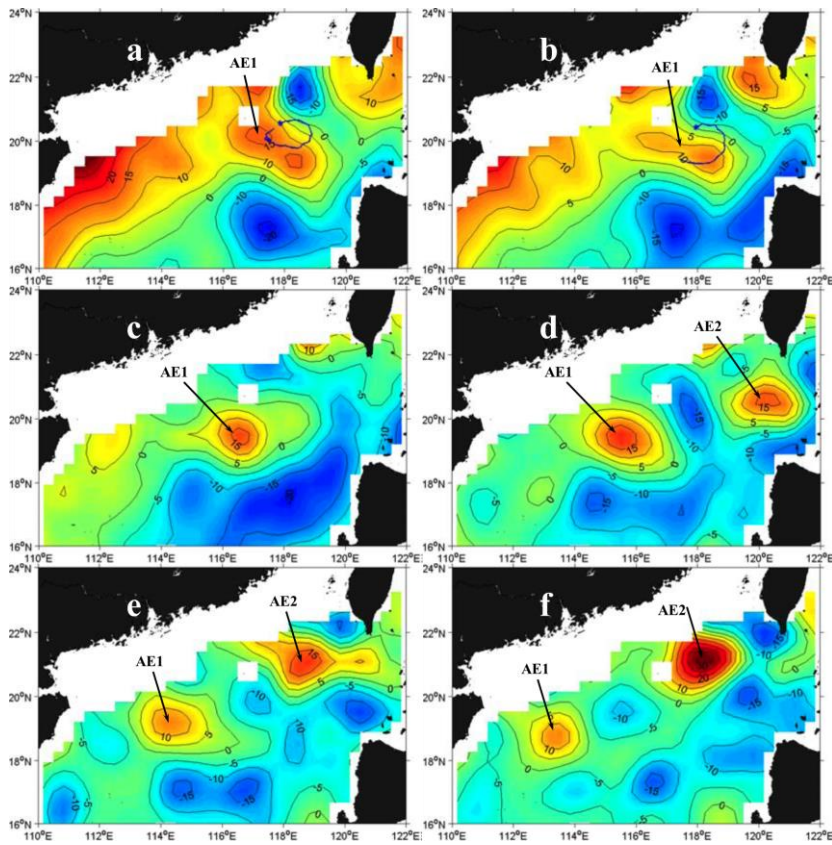
538



539

540 Fig. 2 Annual mean standard deviation of sea level mesoscale signals (color shading, unit: cm) and
 541 propagation velocities of the signals (vectors) derived from (a) altimeter observations; (b) OFES
 542 simulations. From Zhuang et al. (2010).

543

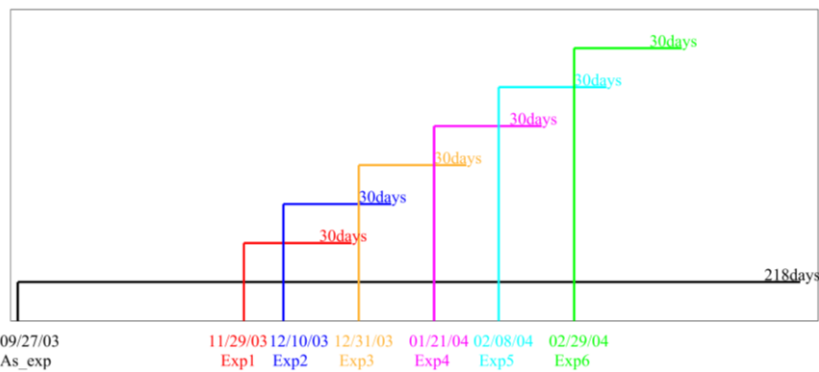


544

545 Fig. 3 Snapshots of SLA from satellite remote sensing datasets. Buoy 22918 trajectory (blue lines,

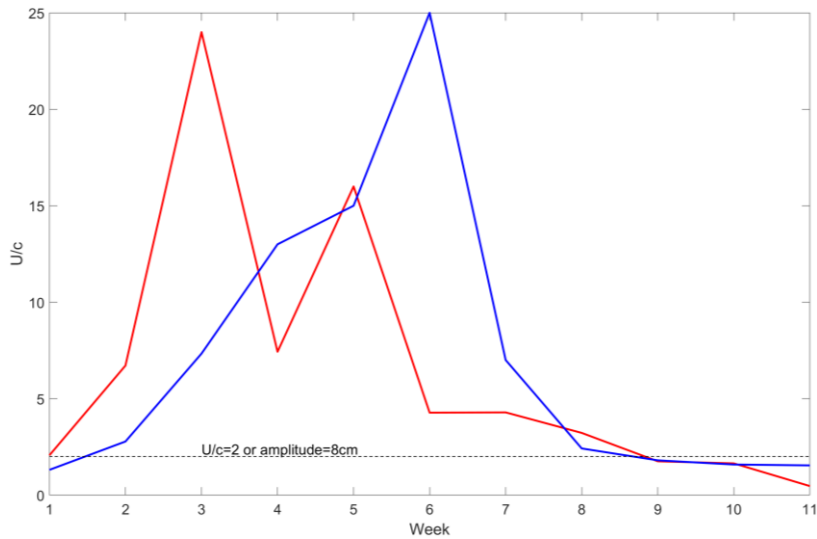
546 blue asterisk represents the initial position of buoy, as in Fig. 4) (a) from December 4-15, 2003
 547 superposed on SLA field on December 10, 2003; (b) from December 16-23, 2003 superposed on
 548 SLA field on December 17, 2003; SLA field on (c) January 7, 2004; (d) January 21, 2004; (e)
 549 February 4, 2004; (f) February 18, 2004. From Wang et al. (2008).

550



551

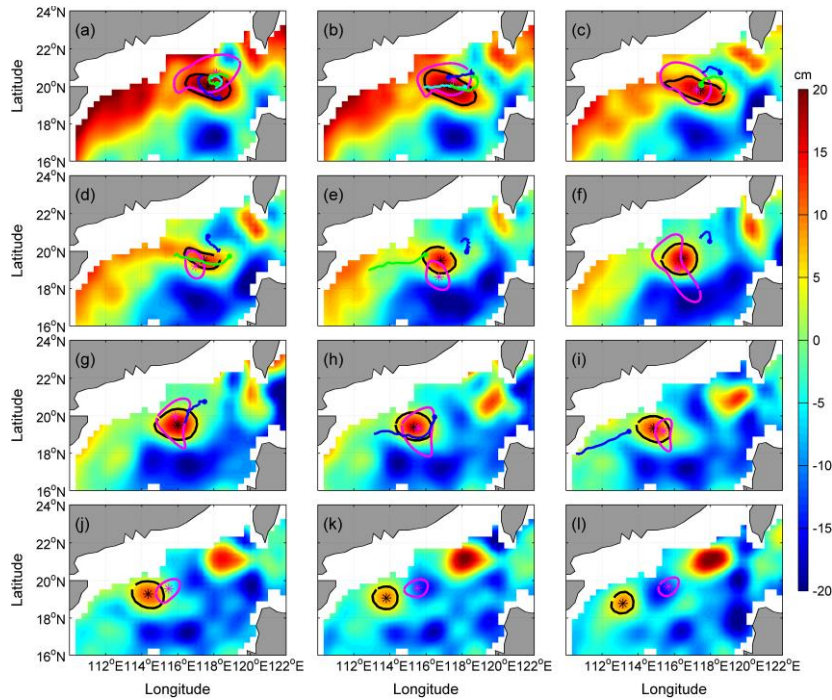
552 Fig. 4 The settings of assimilation and six forecast experiments, including the start and end date.



553

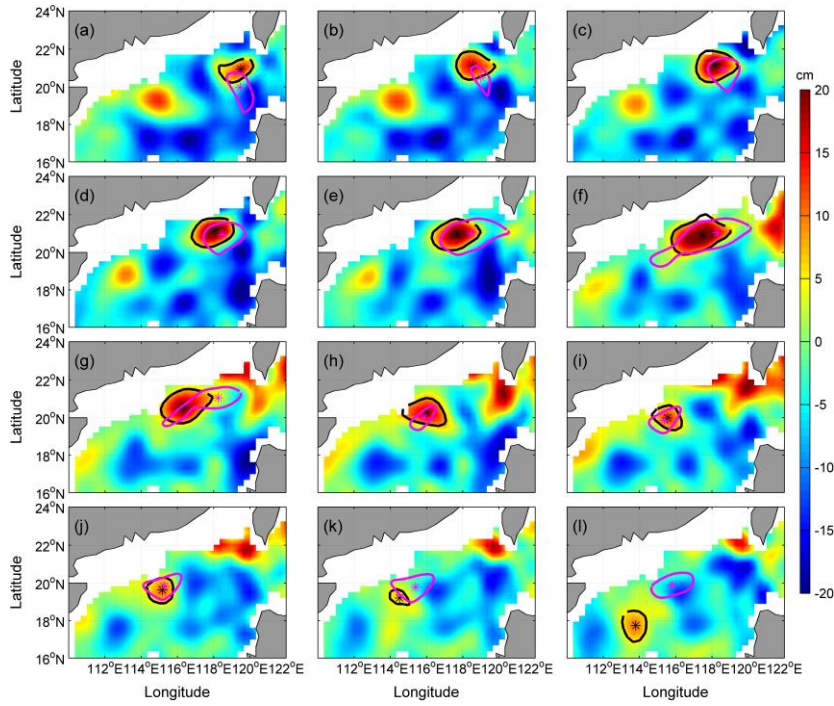
554 Fig. 5 The advective nonlinearity parameter U/c (ANP). The thick red (blue) curve indicates the
 555 ANP of the observed (As_exp experiment) of AE2, the dash line indicates the value of eddy
 556 amplitude at 8 cm or the ANP greater than 2.

557



558

559 Fig. 6 Comparisons of AEI derived from weekly SLA of assimilation results and observation from
 560 satellite remote sensing during the period of December 2003~February 2004. Background color is
 561 SLA, "*" mark and closed lines indicated the center position and the outermost closed isline of
 562 AEI, respectively, the black is from satellite observation SLA, the pink is from assimilation SLA.
 563 The cyan, green and blue solid circle lines indicated the start positions and trajectories of number
 564 22517, 22918 and 22610 drifter buoys, respectively. (a)-(l) is SLA on the 3rd of December 2003~
 565 the 18th of February 2004, respectively. Unit: cm.



566

567 Fig. 7 The same as figure 4, But for AE2, the corresponding period is January 28th, 2003~April 14th, 20

568

569

570

571

572 **Tables:**

573

574

575 Table 1 The amplitude of AE1 and AE2 derived from observation SLA and the assimilation SLA, and distance of eddy centers between the observation SLA's and
576 assimilation SLA's.

Weekly		1(2003/12/3)	2	3	4	5	6	7	8	9	10	11	12	
AE1	Distance (km)		94	45	26	62	98	70	54	30	63	131	199	298
	Amplitude(cm)	Observed	8	10	9	8	8	13	13	11	8	8	4	6
		Assimilated	18	12	11	6	5	4	5	6	2	3	3	2
Weekly		1(2004/1/28)	2	3	4	5	6	7	8	9	10	11	12	
AE2	Distance (km)		107	83	67	57	85	91	221	36	26	26	117	328
	Amplitude(cm)	Observed	7	12	18	17	17	16	15	10	7	6	N/A	6
		Assimilated	3	2	5	6	10	8	4	8	9	4	5	6

577

578

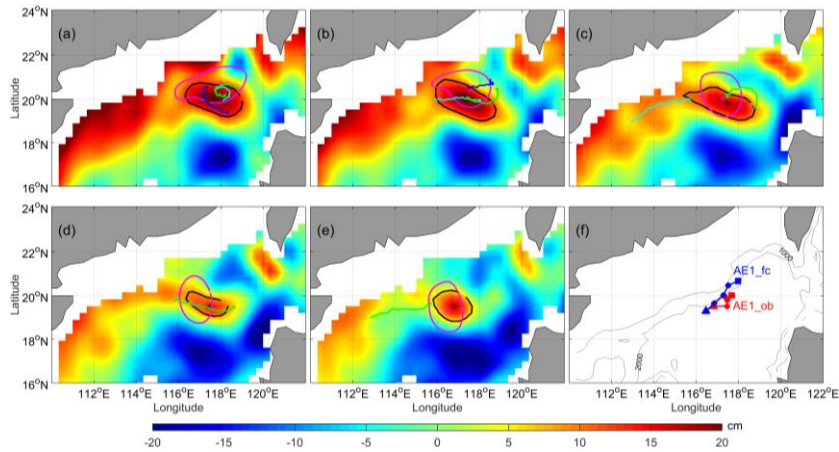
579

580 Table 2 The amplitude of AE1 and AE2 derived from observation SLA and the six forecast SLA,
 581 and distance of eddy centers between the observation SLA's and forecast SLA's.

Weekly		1	2	3	4	5		
Exp1	Distance (km)		80	58	32	68	47	
	Amplitude (cm)	Observed	8	10	9	8	8	
		Forecasted	14	12	14	11	12	
Exp2	Distance (km)		57	22	63	51	113	
	Amplitude (cm)	Observed	10	9	8	8	13	
		Forecasted	12	11	6	8	10	
Exp3	Distance (km)		134	85	111	130	124	
	Amplitude (cm)	Observed	13	13	11	8	8	
		Forecasted	2	3	3	3	N/A	
Exp4	AE1	Distance (km)		32	58	111	161	231
		Amplitude (cm)	Observed	11	8	8	4	6
			Forecasted	4	2	2	2	N/A
	AE2	Distance (km)		N/A	N/A	132	95	81
		Amplitude (cm)	Observed	N/A	N/A	12	18	17
			Forecasted	N/A	N/A	N/A	6	9
Exp5	AE1	Distance (km)		188	274	287	405	503
		Amplitude (cm)	Observed	4	6	2	N/A	N/A
			Forecasted	2	2	2	2	2
	AE2	Distance (km)		69	77	102	95	226
		Amplitude (cm)	Observed	18	17	17	16	15
			Forecasted	5	7	6	6	9
Exp6	AE2	Distance (km)		91	227	277	339	453
		Amplitude (cm)	Observed	16	15	10	7	6
			Forecasted	7	9	6	4	6

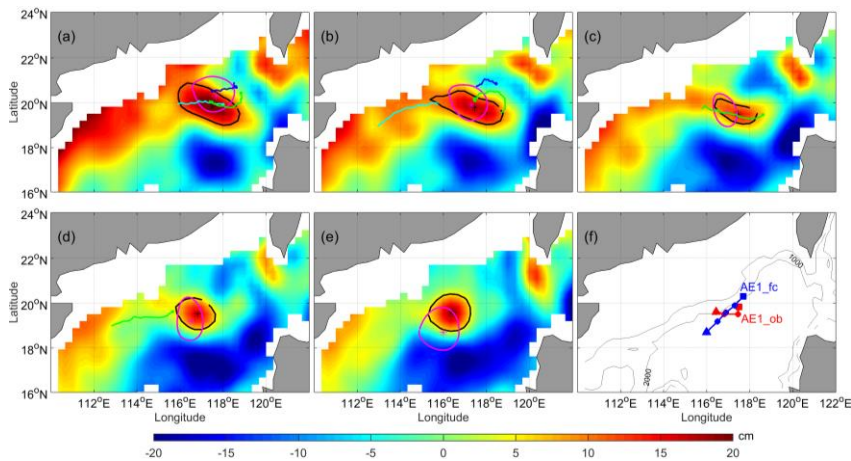
582

583



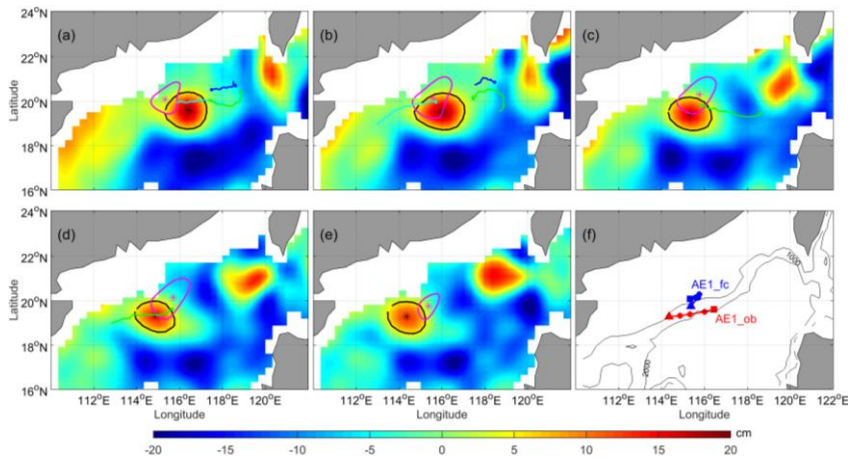
584

585 Fig. 8 Comparison of AEI of Exp1 and observation, and trajectories of drifter buoys during the 29th
586 of November 2003 and the 29th of December 2004. The cyan, green and blue solid circle dots and
587 lines indicated the start positions and trajectories of number 22917, 22918 and 22610 drift buoys
588 during the corresponding period, respectively. Where, the red (blue) dotted line in (f) is the moving
589 path of AE1 derived from observation (forecast) SLA during the experiment period, the square
590 (triangle) represents the start (end) position.



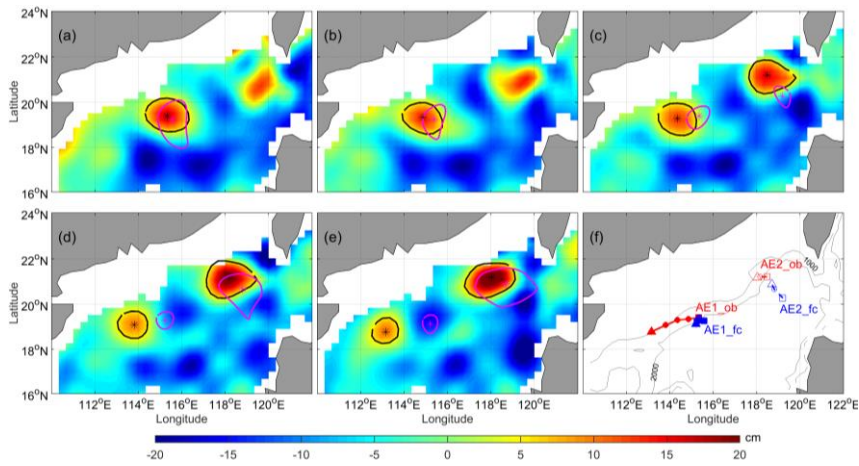
591

592 Fig. 9 Same as figure 8, but for Exp2, the experiment period is the 10th of December 2003 to the 9th of
593 January 2004.



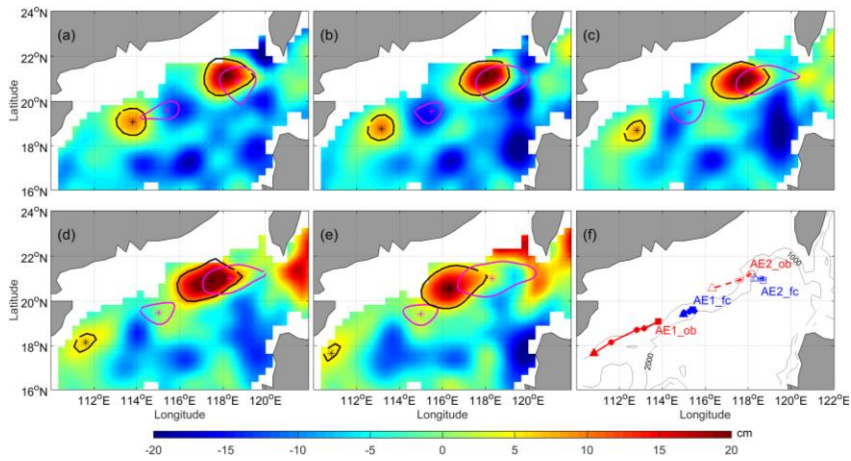
594

595 Fig. 10 Same as figure 9, but for Exp3, the experiment period is the 31st of December 2003 to the 30^h of
 596 January 2004.

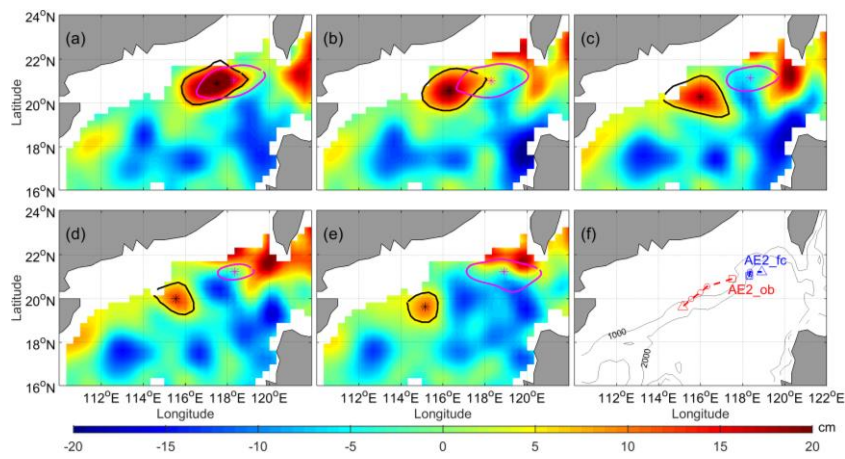


597

598 Fig. 11 Same as figure 8, but for Exp4, where, there (blue) dotted line in (f) is the observation (forecast)
 599 moving path of AE1 and AE2 the red solid (dashed) lines and solid (hollow) circle derived from
 600 observation SLA for AE1 (AE2), the blue solid (dashed) lines and solid (hollow) circle derived from
 601 forecast SLA during the 21st of January 2004 to the 20^h of February 2004.

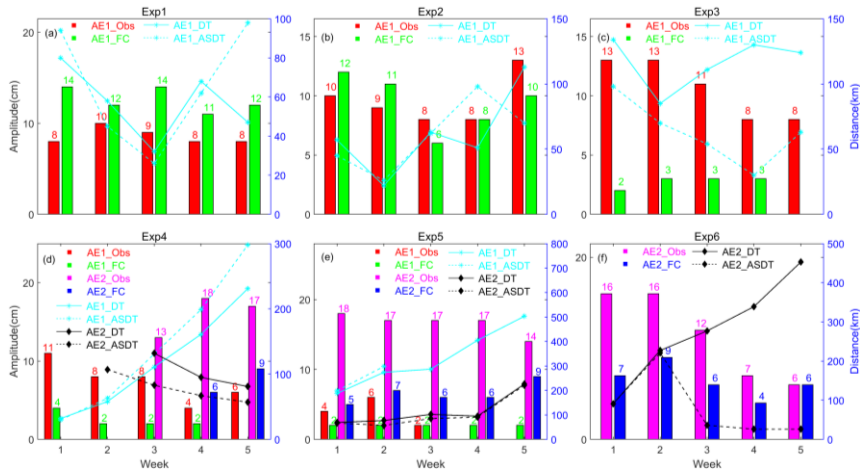


602
 603 Fig. 12 Same as figure 11, but for Exp5, the experiment period is the 8th of February 2004 to the 10th of
 604 March 2004.



606
 607 Fig. 13 Same as figure 11, but for Exp6 and AE2, the experiment period is the 29th of February 2004 to
 608 the 30th of March 2004.

609



610

611 Fig. 14 The amplitude of AE1 and AE2 derived from observation SLA and the six forecast SLA,
 612 and distance of eddy centers between the observation, assimilation and forecast SLA's, respectively.
 613 The red and green histograms indicated the AE1 amplitudes from observation and prediction
 614 respectively. The pink and blue histograms expressed the AE2 amplitudes from observation and
 615 prediction respectively. The cyan star solid (dash) line shows the distance of the center between
 616 observation and prediction (assimilation) AE1. The black diamond solid (dash) line shows the
 617 distance of the center between observation and prediction (assimilation) AE2.

618